JOURNAL OF VIROLOGY, May 1997, p. 3799–3810 Vol. 71, No. 5
0022-538X/97/$04.00+0

Engineering of Homologous Recombination Hotspots with AU-Rich Sequences in Brome Mosaic Virus

PETER D. NAGY† AND JOZEF J. BUJARSKI*

Plant Molecular Biology Center and Department of Biological Sciences, Northern Illinois University, De Kalb, Illinois 60115

Received 8 August 1996/Accepted 1 February 1997

Previously, we observed that crossovers sites of RNA recombinants clustered within or close to AU-rich regions during genetic recombination in brome mosaic bromovirus (BMV) (P. D. Nagy and J. J. Bujarski. J. Virol. 70:415–426, 1996). To test whether AU-rich sequences can facilitate homologous recombination, AU-rich sequences were introduced into parental BMV RNAs (RNA2 and RNA3). These insertions created a homologous RNA2-RNA3 recombination hotspot. Two other AU-rich sequences also supported high-frequency homologous recombination if a common sequence with high or average G/C content was present immediately upstream of the AU-rich element. Homologous RNA recombination did not require any additional sequence motifs or RNA structures and was position nonspecific within the 3′ noncoding region. These results suggest that nucleotide content (i.e., the presence of common 5′ GC-rich or moderately AU-rich and 3′ AU-rich regions) is the important factor that determines the sites of homologous recombination. A mechanism that involves replicase switching during synthesis of positive-sense RNA strands is presented to explain the observed results.

RNA-RNA recombination can facilitate the appearance of new viral RNA genomes either through the joining of different functional modules within the virus genome or incorporating host sequences into the virus genome (13, 14, 17, 41, 45). In addition, RNA recombination can provide the means for viruses to repair defects of RNA replication by replacing mutated sequences with wild-type (wt) regions (7, 8, 21, 26, 42). RNA recombination can also increase sequence variability in a virus population through imprecise crosses and thereby contribute to the maintenance of the quasispecies nature of viruses (9, 29, 30).

Several types of studies suggested that RNA-RNA recombination can utilize various kinds of replicase-driven template-switching mechanisms (7, 8, 10, 11, 16, 17, 21, 40, 43), and experimental evidence that supports a template-switching mechanism was obtained for picornavirus (18) and bromovirus recombination (29). RNA sequences and structures that facilitate viral RNA-RNA recombination have been investigated in several plant virus systems such as brome mosaic bromovirus (BMV), turnip crinkle carmovirus (TCV), and tomato bushy stunt tombusvirus (5, 7–11, 26–30, 40, 43). For example, it was shown that local heteroduplex structures that formed between recombining RNAs promoted the crossover events and targeted the sites of nonhomologous recombination in BMV (27). In TCV, recombination occurred within one of three promoter-like motifs that can form hairpin-loop structures (9, 11). It was proposed that the TCV replicase can recognize these hairpin-loop structures during the template-switching events. Recombination site selection in TBSV was influenced by the presence of a stable secondary structure that caused a shift in the location of junctions toward less structured regions (43). Sequence and structure requirements of RNA recombination are less well defined for other viruses. For instance, formation of local heteroduplexes at regions of complementarity was proposed to facilitate the selection of homologous junction sites in picornavirus recombinants (38) and during the formation of defective interfering RNAs in bromo- and tombusviruses (33, 43). In addition, it was predicted that negative-sense RNA provides the means by which the two parental positive-sense RNAs are brought into proximity during recombination events in bromoviruses (8) and in poliovirus (20). RNA recombination may be analogous to transcription priming during the subgenomic RNA synthesis in coronaviruses that can lead to the heterogeneity of leader-mRNA fusions (46).

BMV represents a well-described, model RNA-RNA recombination system. Each of three positive-stranded genomic RNAs of BMV contains approximately 200 nucleotides (nt) of homologous 3′ noncoding sequence (2). The 3′ end of this region can form a tRNA-like structure that is involved in the initiation of minus-strand synthesis (reviewed in reference 1). Both homologous and, less frequently, nonhomologous recombination processes in BMV have been observed (5, 6, 26–30, 35–37). While nonhomologous recombination was facilitated by local sequence complementarity (27), homologous recombination required local sequence homology among the recombining BMV RNAs (28). As little as 5 nt of sequence identity supported RNA recombination, while similar regions of 15 nt or longer were required for high-frequency homologous recombination (28). In addition to the length of the similar region, the extent of sequence identity influenced the efficiency of homologous recombination (28). Some of the homologous recombination events were imprecise, leading to duplication and/or deletion of parental sequences, and some crossover sites contained mismatched or nontemplate residues (30).

However, not all homologous sequences were capable of targeting crossover events (27, 31). This observation argues that sequence homology by itself is not sufficient, and additional information must be present on the RNA templates to induce homologous recombination. One possibility is that the AU content of the homologous region is an important factor, since both precise and imprecise homologous crossover events were frequently mapped to the AU-rich regions on BMV

* Corresponding author. Mailing address: Plant Molecular Biology Center, Northern Illinois University, Montgomery Hall, De Kalb, IL 60115. Phone: (815) 753-0601. Fax: (815) 753-7855. E-mail: t80jjb1@wpo.cso.niu.edu.

† Present address: Department of Biochemistry and Molecular Biology, University of Massachusetts, Amherst, MA 01003.

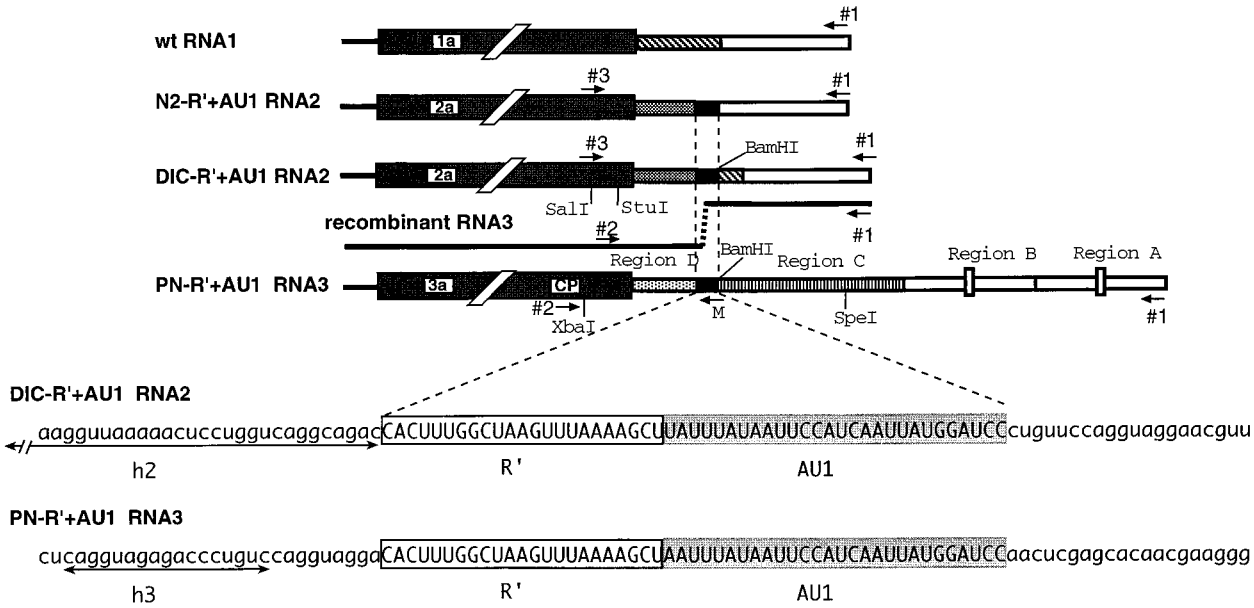

FIG. 1. Schematic representation of the 3′ noncoding regions of wt BMV RNA1, N2-R′+AU1 and DIC-R′+AU1 RNA2, and PN-R′+AU1 RNA3 constructs used for testing the effect of AU-rich sequences on homologous recombination. The PN-R′+AU1 RNA3 molecule contains a ~1,250-nt-long, chimeric 3′ noncoding region that consists of four elements (regions A to D). Region A contains wt RNA3 sequences located between positions 1 and 162 (counted from the 3′ end [2]) and an upstream RNA1-derived region (positions 163 to 236 in wt RNA1). Region B contains sequences located between positions 7 and 200 in wt RNA3. Both regions A and B have a deletion (positions 81 to 100 in wt RNA3; shown by small rectangular boxes). Region C has a 765-nt sequence derived from cowpea chlorotic mottle bromovirus RNA3 (positions 24 to 788, counted from the 3′ end [3]). Region D (shown as a dotted box) contains wt RNA3 sequences located between positions 220 and 297. PN-R′+AU1 RNA3 also contains a 23-nt-long sequence (designated as R′; positions 196 to 219 in wt RNA2) and a 28-nt artificial AU-rich region (designated AU1). The locations of the restriction sites are indicated; oligonucleotide primers used for PCR are shown by short horizontal, numbered arrows. Arrow M depicts the position of the following mutagenesis oligodeoxynucleotides: 12, 65, 90, 91, 92, 95, 96, 128, 147, 148, 184, 192, and 203 (see Materials and Methods). N2-R′+AU1 and DIC-R′+AU1 RNA2s also contain R′ and the AU1 (enclosed within dashed lines). In both RNA2 mutants, the 3′ noncoding sequence upstream of the R′+AU1 region is derived from wt RNA2 (positions 220 to 293). N2-R′+AU1 RNA2 has the downstream 3′ noncoding sequence derived from wt RNA2 (positions 1 to 195), while the corresponding region in DIC-R′+AU1 RNA2 is derived from wt RNA1 (positions 1 to 236). The h2 and h3 sequences are depicted by horizontal arrows.

RNAs (28, 29). In this report, we examine the role of AU-rich sequences in homologous recombination of BMV.

MATERIALS AND METHODS

Materials. Plasmids pB1TP3, pB2TP5, and pB3TP7 (15) were used as templates to prepare in vitro transcripts equivalent to BMV RNA components 1, 2, and 3, respectively. Plasmids PN-H65 (PN-R′) and DIC-0 were previously described (27, 28). Construction of DIC-GC1, DIC-GC3, DIC-h3, DIC-H39, PN-GC1, PN-GC3, and PN-h2 will be described elsewhere (31). Moloney murine leukemia virus reverse transcriptase was from Gibco BRL (Gaithersburg, Md.), *Taq* DNA polymerase, restriction enzymes, and T7 RNA polymerase were from Promega Corp. (Madison, Wis.), and a Sequenase kit was from U.S. Biochemical Corporation (Cleveland, Ohio). The following oligonucleotide primers were used in this study (the unique *Eco*RI and *Bam*HI sites are underlined, and alternative bases are shown in parentheses): 1, 5′-CAGTGAATTCTGGTCTC TTTTAGAGATTTACAG-3′; 2, 5′-CTGAAGCAGTGCCTGCTAAGGCGGT C-3′; 3, 5′-AGAAGGTCGACGATTACGCTACC-3′; 12, 5′-CAGTGGATCCA TAATTGATGGAATTATAAATCGACAGGGTCTCTACCTGCCTGACCA GGAG-3′; 65, 5′-CAGTGGATCCATAATTGATGGAATTATAAATGGACA GGGTCTCTACC-3′; 90, 5′-CAGTGGATCCATAATTGAT(GC)(GA)AATT ATAAA(CT)AAGTGGTCTGCCTG-3′; 91, 5′-CAGTGGATCCATAATTGA T(GC)(GA)AATTATAAA(CT)AAGTGTCCTACCTG-3′; 92, 5′-CAGTGGA TCCATAATTGATGGAATTATAAAT(TA)AGCTTTTAA(CA)CTTAGCC -3′; 128, 5′-CAGTGGATCC(AC)CACTTTGGCTAAGGTTAAAAGC-3′; 147, 5′-CAGTGGATCCTTTTTTTTTTTTTTTTTTT(AT)AGCTTTTAACCTTA GCC-3′; 148, 5′-CAGTGGATCCATAATTGATGGAAAAAAAAAA(AT)AG CTTTTAACCTTAGCC-3′; 192, 5′-CAGTGGATCCATTTATAATTGA(GT)GAATTATAAA(AG)AGCTTTTAACCTTAGCC-3′; and 203, 5′-CAGTGGAT CCTTTTAATTTTAATTTTAATTTTAA(AT)AGCTTTTAA(CA)CTTAGCC-3′.

Engineering of parental constructs. PN series plasmids (described below) are derivatives of pB3TP7, while DIC and N2 series plasmids are derivatives of pB2TP5. To obtain plasmids PN-R′+AU1, PN-R′+AU2, PN-R′+AU3, PN-AU1, PN-AU1N, and PN-R′+A20, a ~200-bp-long 3′ cDNA fragment derived from PN-H65, a plasmid containing full-length cDNA of BMV RNA3 with a modified 3′ end that included R′ (28), was amplified by PCR using primer 2 and one of the following mutagenesis primers: 92, 192, 203, 65, 91, and 147, respectively (shown as primer M in Fig. 1). The amplified cDNA fragment was digested with *Bam*HI and *Xba*I and then used to replace the 3′ 166-bp *Bam*HI-*Xba*I fragment in PN-H65. The corresponding plasmids were selected by sequence analysis. A similar approach was used to generate constructs DIC-R′+AU1, DIC-R′+AU2, DIC-R′+AU3, DIC-AU1, DIC-h3+AU1, and DIC-R′+AUU with primer 3 and one of the following mutagenesis primers: 92, 192, 203, 90, 12, and 148. The amplified cDNA fragment was digested with *Bam*HI and *Stu*I and then used to replace the corresponding fragment in DIC-0 (30). N2+AU1 and N2+R′+AU1 constructs were obtained after the following steps. DIC-AU1 and DIC-R′+AU1 constructs were digested with *Bam*HI and treated with T4 DNA polymerase. The enzymes were inactivated at 75°C for 10 min, and the DNA was digested with *Eco*RI. The large fragments that included the vector sequences were isolated from agarose gels and ligated with the ~200-bp *Hin*dIII (after treatment with T4 DNA polymerase)-*Eco*RI fragment of pB2TP5.

To generate DIC-AU1+R′ and PN-AU1+R′, the 3′-end sequences were amplified by PCR using primers 128 plus primers 3 and 2, respectively. The PCR products were digested with either *Bam*HI-*Stu*I or *Bam*HI-*Xba*I and ligated to the corresponding sites in DIC-AU1 and PN-AU1N, respectively.

Constructs DIC-AU1+AU2, DIC-GC1+AU1, and DIC-GC3+AU1 were obtained by digesting DIC-AU1, DIC-GC1, and DIC-GC3, respectively, with *Bam*HI, followed by filling in the ends with T4 DNA polymerase and deoxynucleotides, heat inactivating the polymerase (as described above), and digesting it with *Eco*RI. The large fragments that included the vector sequences were isolated from agarose gels and ligated with the ~260-bp *Hin*dIII (after filling in the end with T4 DNA polymerase and deoxynucleotides)-*Eco*RI fragment of DIC-R′+AU1. Basically, the same approach was used to construct PN-AU1+AU2, PN-GC1+AU1 and PN-GC3+AU1, starting with PN-AU1N, PN-GC1 and PN-GC3, respectively, and using the small *Hin*dIII-*Eco*RI fragment of PN-R′+AU1.

To obtain PN-h2+AU1 RNA3 construct, a ~150-bp fragment was amplified from DIC-AU1 by PCR with primers 3 and 90. The resulting PCR product was digested with *Alu*I and *Bam*HI and then ligated between *Eco*RV-*Bam*HI sites in PN-H149, which contained a unique *Eco*RV site corresponding to position 238 (from the 3′ end in pB3TP7) and the standard *Bam*HI-*Eco*RI region of PN-H65.

The entire PCR-amplified regions in all of these constructs were sequenced to confirm the mutations introduced.

Construction of full-length recombinant RNA3 clones. Full-length cDNA clones of five different types of homologous recombinants (rec-R′, rec-AU1N, rec-AU1, rec-R′+AU1, and rec-R′+AU3) were constructed by replacing the 1,160-bp *Bam*HI-*Eco*RI inserts of PN-R′ (Fig. 2A), PN-AU1N (Fig. 3B), PN-

AU1 (Fig. 3A), PN-R′+AU1 (Fig. 1 and 2B), and PN-R′+AU3 (Fig. 2E), respectively, with the corresponding 241-bp fragment of DIC-R′+AU1 (Fig. 1).

Whole-plant inoculation, Northern blot analysis, reverse transcription (RT)-PCR amplification, cloning, and sequencing. Leaves of *Chenopodium quinoa* were inoculated with a mixture of the transcribed BMV RNA1 to RNA3 as described by Nagy and Bujarski (26, 28). Briefly, a mixture of ~4 μg of each transcript in 15 μl of inoculation buffer (10 mM Tris [pH 8.0], 1 mM EDTA, 0.1% Celite, 0.1% bentonite) was used to inoculate one fully expanded leaf. A total of six leaves were inoculated for each RNA3 mutant. Each experiment was repeated twice or more. Total RNA was extracted (as described in reference 26) 14 days postinoculation. In the case of reconstructed RNA3 recombinants, total RNA was obtained 10 days postinoculation. One-fifth of the total RNA extract was separated by electrophoresis in a 1% agarose gel, transferred to a Hybond N+ (Amersham) nylon membrane, and analyzed by Northern blot analysis. Hybridization to a 200-nt ^{32}P-radiolabeled BMV RNA probe that is specific for the 3′ ends of positive strands of all RNAs was done as described by Kroner et al. (19).

Total RNA was also used for RT-PCR amplification, exactly as described previously (35). The 3′ end of the progeny RNA3 was amplified by using primers 1 and 2 (Fig. 1). Standard electrophoresis in 1.5% agarose gels was used to estimate the sizes of the cDNA products (39). The cDNA fragments were digested with restriction enzymes *Eco*RI and *Xba*I and ligated into the *Eco*RI and *Xba*I cloning sites in the pGEM3zf(−) cloning vector (Promega). Sites of crossovers were determined by sequencing with Sequenase as specified by the manufacturer (U.S. Biochemical).

We have developed an experimental strategy to clone a representative recombinant RNA3 from a given lesion and also to ensure that the cloned RT-PCR products are independent (see for details, reference 29). Briefly, local lesions located far apart from each other on the inoculated leaves were cut out separately (only one or two lesions were chosen on each leaf). In addition, a single RT-PCR clone from a given local lesion sample was sequenced. Thus, RT-PCR-amplified sibling clones were not scored in this study. This was important, since during the preliminary studies we demonstrated that five RT-PCR clones derived from the same lesion had identical sequence in the crossover region, while separate lesions accumulated recombinant RNA3s with different junction sites.

Analysis of the stability of added sequences during infection. The 3′ sequences of parental RNA2 constructs were amplified by RT-PCR using primers 1 and 3 with total RNA extracted from separate local lesions on *C. quinoa* 14 days after inoculation from DIC-R′+AU1 RNA2 and PN-R′+AU1 RNA3 infections. Thereafter, the amplified cDNA was digested with *Sal*I and *Eco*RI, followed by ligation into the corresponding sites in pGEM3zf(−). The stability of AU1 sequences in the parental RNA3 progeny was analyzed by RT-PCR, cloning, and sequencing as described above for the RNA3 recombinants. Not all of the lesions contained parental RNA3 at the time of analysis, because the novel recombinant RNA3 can outcompete the parental RNA3 molecules. The clones were generated only from those local lesions that contained the parental-size RNA3 (as judged by the size of the RT-PCR-amplified cDNA).

RESULTS

Different AU-rich inserts create homologous recombination hotspots. Most of the studies of recombination in BMV have used RNA3 mutants, since this RNA segment is dispensable for BMV RNA replication (5, 6, 26–30, 35–37). The most frequently used host system is *C. quinoa* or *C. hybridum*, on which the mutated parental BMV RNA3 in the presence of RNA1 and RNA2 induces small local lesions, each of which represents an independent infection (see Materials and Methods). Recombination frequency or incidence was measured by assaying the percentage of local lesions that accumulated homologous recombinants.

Previously, we found that both precise and imprecise homologous recombination occurred frequently within or adjacent to AU-rich stretches in the 3′ noncoding sequence that is common between BMV RNA2 and RNA3 (28, 30). To determine if AU-rich sequences can serve as homologous recombination hotspots, we used derivatives of BMV RNA2 and RNA3 constructs that have modified 3′ noncoding regions. In particular, the RNA3 construct designated PN-R′ RNA3 contains a 23-nt insert (R′) that was similar to the corresponding region in the RNA2 construct designated DIC-R′ RNA2 (Fig. 1 and 2A). The extended 3′ noncoding region in the RNA3 constructs rendered the parental RNA3s less competitive than the shorter recombinant RNA3s, thus allowing the accumulation of de novo recombinants in local lesions (26–30). In the RNA2 constructs, the 3′-terminal 196 nt have been replaced with the 3′-terminal 236 nt of wt RNA1 in order to separate R′ from the 3′-terminal RNA replication promoter (30). We found that this particular 3′ sequence arrangement allowed the extensive modification of R′ without debilitating the replication of the given RNA (see below). Homologous RNA2-RNA3 recombinants with crossover events within the common (i.e., located on both RNA2 and RNA3) R′ region were identified in 39% of local lesions on *C. quinoa* leaves upon coinoculation of wt RNA1, DIC-R′ RNA2, and PN-R′ RNA3 (Fig. 2A). An additional 19% of local lesions contained nontargeted RNA1-RNA3 recombinants. The genomic RNAs of these recombinants accumulated to a lower level and later (14 to 21 daypostinoculation) than the above-mentioned homologous RNA2-RNA3 recombinants (8 to 14 daypostinoculation). The remaining lesions contained low concentrations of the parental RNA3 molecules (data not shown).

To determine if different AU-rich sequences can support homologous recombination, a synthetic 28-nt AU-rich sequence (designated AU1) was inserted directly downstream of R′ in both DIC-R′ RNA2 and PN-R′ RNA3 vectors (constructs DIC-R′+AU1 RNA2 and PN-R′+AU1 RNA3 [Fig. 1]). Sequencing of the 3′ end of the progeny of the parental RNAs (see Materials and Methods) revealed that the 3′ regions were maintained in the parental RNA2 and RNA3 constructs in plants (data not shown). Thus, the introduced AU1 sequences were available for recombination in the local lesions. The presence of the downstream AU1 increased the incidence of RNA2-RNA3 homologous recombination in local lesions from 39 to 75% (Fig. 2B). Of 27 homologous recombinants analyzed, 24 had the junction sites within AU1 and 3 had junction sites in R′. The observed shift in the site of recombination into AU1 cannot be attributed to a difference in sequence length, because the sizes of R′ and AU1 are comparable. In contrast, insertion of AU1 immediately upstream of R′ (constructs DIC-AU1+R′ RNA2 and PN-AU1+R′ RNA3) gave homologous RNA2-RNA3 recombinants in 47% of the local lesions tested. In this case, the crossover events occurred more frequently within R′ (33%) than within AU1 (14%). Apparently, the upstream AU1 did not change significantly the overall recombination activity of R′ (compare Fig. 2A and C; more than a 20% difference in recombination frequency between different combinations was considered significant during this work based on standard deviation). In addition, the increased length of the common region (due to the addition of AU1) in DIC-AU1+R′ RNA2 and PN-AU1+R′ RNA3, compared to DIC-R′ RNA2 and PN-R′ RNA3, did not substantially affect the overall incidences of homologous recombination (39% without AU1, compared with 47% with AU1). This result argues that the increased recombination incidence (from 39 to 75%), observed with constructs carrying the downstream AU1 cannot be attributed simply to the presence of the common AU1 but rather must also reflect the position of these sequences within the RNAs (Fig. 2A and B; see also Discussion).

To further test the role of AU-rich sequences in homologous recombination, two other artificial AU-rich sequences, designated AU2 and AU3, were introduced separately downstream of R′ in RNA2 (constructs DIC-R′+AU2 and DIC-R′+AU3) and RNA3 (constructs PN-R′+AU2 and PN-R′+AU3). While the A/U content of AU1 was 75%, the A/U contents of AU2 and AU3 were 73 and 87%, respectively. Figures 2D and E show that infections with either DIC-R′+AU2 RNA2 and PN-R′+AU2 RNA3 or DIC-R′+AU3 RNA2 and PN-R′+AU3 RNA3 generated homologous RNA2-RNA3 recombinants in 75 and 83% of local lesions, respectively. This result confirmed

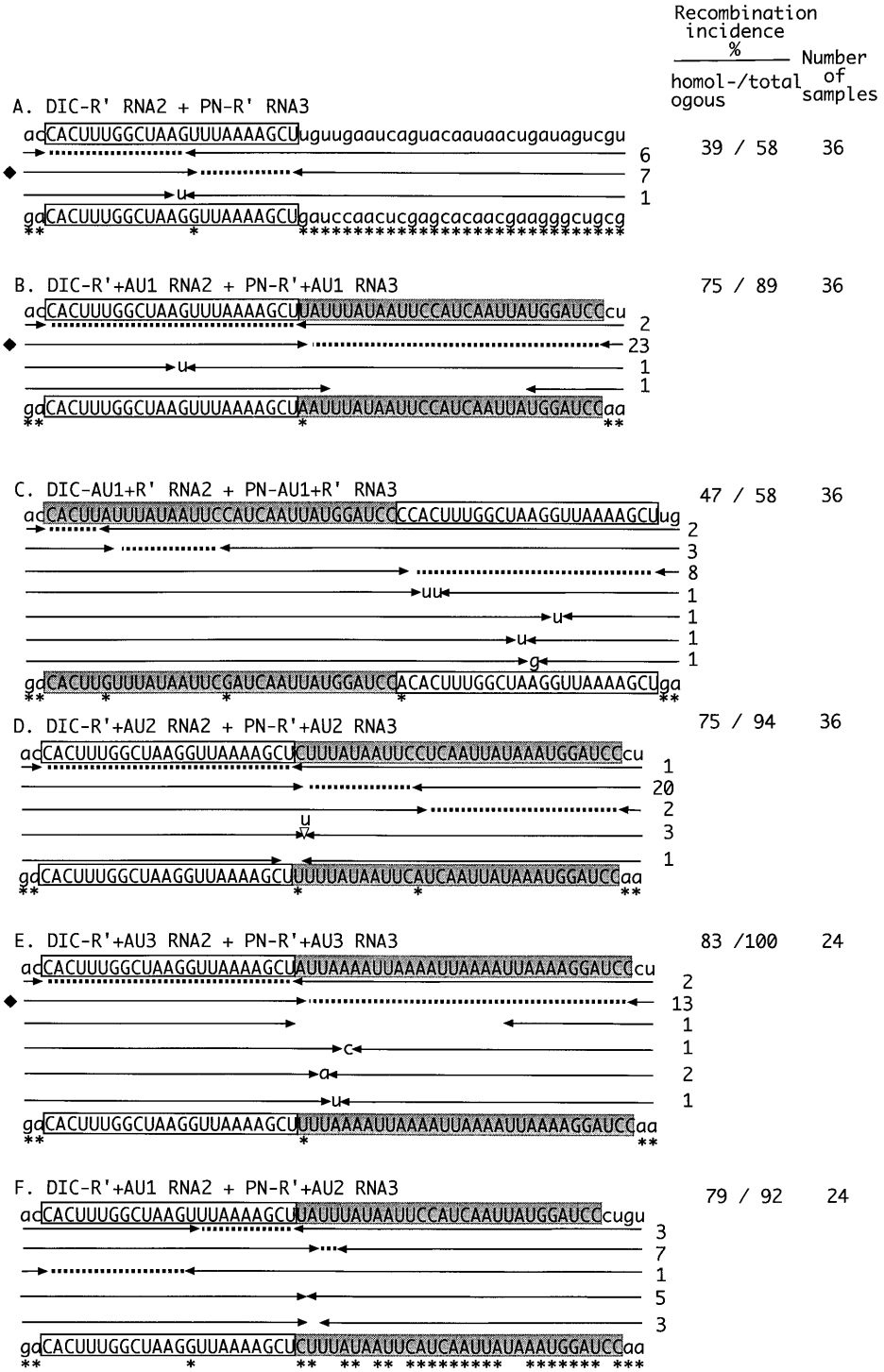

FIG. 2. Diagram summarizing the recombination frequencies and distribution of crossover sites in the homologous RNA2-RNA3 recombinants isolated from infections with wt RNA1, DIC series of RNA2, and PN series of RNA3 constructs. Homologous RNA2 and RNA3 positive-sense sequences are shown on the top and bottom lines, respectively. Capital letters depict the homologous R′ (boxed) and the AU-rich segment (shaded). Marker mutations are indicated by asterisks under the RNA3 sequences. Each recombinant contains 3′-terminal sequences derived from RNA2 on the right side and 5′ sequences from RNA3 on the left side (as shown schematically in Fig. 1). Each leftward pointing arrowhead denotes the last nucleotide derived from RNA2, and each rightward pointing arrowhead denotes the first nucleotide derived from RNA3. Dashed lines show ambiguous regions that could be derived from either RNA2 or RNA3 in the precise homologous recombinants. Gaps between opposing arrowheads show deleted nucleotides, whereas sequence insertions are represented by open triangles. Nontemplated nucleotides and nucleotide substitutions generated during the crossover events are shown by lowercase letters between the arrows. The nucleotide sequences in the imprecise recombinants with ambiguous crossovers were arbitrarily placed with the upstream junction. Each entry represents an RNA2-RNA3 recombinant isolated from separate local lesion. The incidence of each RNA3 recombinant is shown by numbers on the right. The percentages of homologous and total (the latter includes both homologous and the background recombinants; see Results) recombination incidence were calculated by sequencing a representative number of cloned recombinant RNA3s as described in reference 26. Those recombinant RNA3s which had been reconstructed (Fig. 6) are marked by filled diamonds. The numbers of analyzed total RNA samples obtained from separate local lesions are shown on the right. Standard deviation was less than 20 for homologous and total recombination incidence in all combinations in Fig. 2 to 5 (not shown). Thus, more than 20% difference in recombination frequency between different combinations was considered significant during this work.

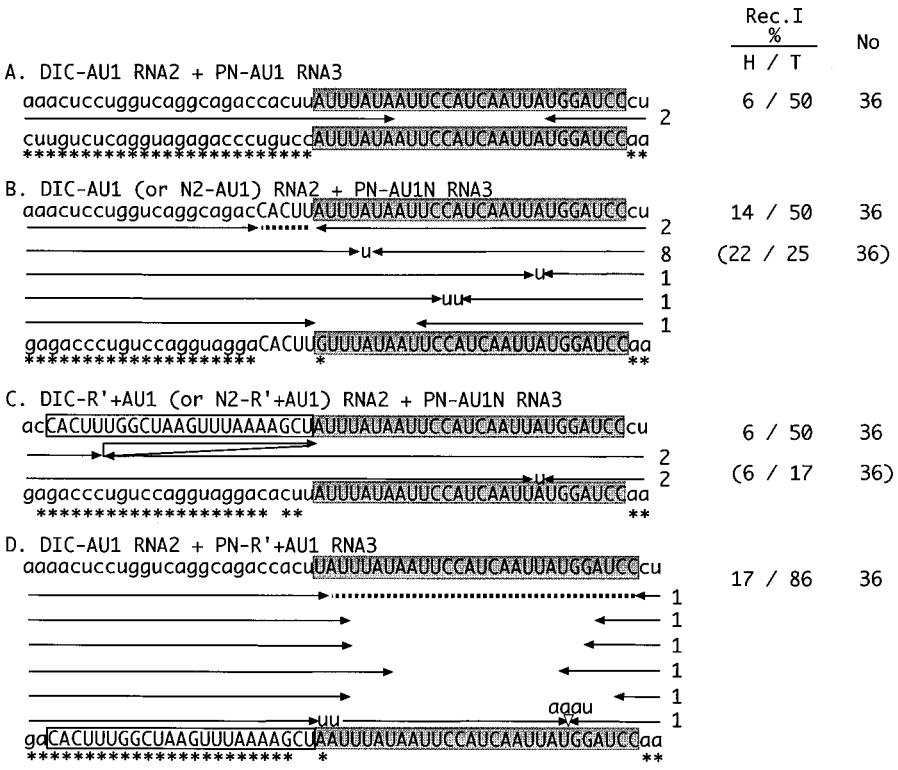

FIG. 3. Incidence of recombination and distribution of crossover sites in homologous recombinant RNA3 molecules obtained with pairs of one of the DIC series of RNA2 and one of the PN series of RNA3 constructs (as shown) that contained the AU-rich sequences but lacked common R′ sequences. Overlapping arrows show sequence duplications in some imprecise recombinants. Recombination incidence obtained with either N2-R′+AU1 or N2-AU1 RNA2 constructs are shown in parentheses (see Results). The total numbers of samples analyzed and other features are as described in the legend to Fig. 2.

that AU-rich sequences that differ in nucleotide composition can facilitate homologous recombination. The crossover events that were identified in the isolated recombinants were mainly within the AU2 and AU3 regions and were concentrated within the 5′ portion of AU-rich sequences (Fig. 2D and E). The clustering of crossover sites in the 5′ portion of the AU-rich region was also observed in infections with RNAs containing different AU-rich segments (DIC-R′+AU1 RNA2 and PN-R′+AU2 RNA3 [Fig. 2F]).

The AU-rich sequences AU1, AU2, and AU3 differed in their predicted (computer-generated) secondary structures. The AU3 sequence was predicted to form the least stable secondary structure (not shown), but it supported slightly higher recombination frequency than AU1 and AU2 (Figs. 2B, D, and E). Also, AU3 supported the highest percentage of imprecise homologous recombination events (i.e., deletions and/or insertions or mismatched or nontemplated nucleotides at the crossover points) compared to AU1 or AU2 (Fig. 2B, D, and E). Thus, no correlation between predicted structural stability and homologous recombination was observed.

Removal of R′ region reduces recombination efficiency within the nearby AU-rich sequences. As described above, different AU-rich sequences when located downstream of R′ increased the recovery of homologous recombinants and constituted recombination hotspots. This finding suggested that R′ might be contributing to the recombination events. For example, R′ may act as an obstacle for the replicase, thus causing the enzyme to switch onto the acceptor RNA within the downstream AU-rich sequence. To test whether R′ was affecting homologous recombination in the downstream AU-rich sequences, R′ was deleted from both RNA2 (designated DIC-AU1 RNA2) and RNA3 (PN-AU1 RNA3) constructs (Fig. 3A). Plants inoculated with DIC-AU1 RNA2 and PN-AU1 RNA3 accumulated homologous recombinants only in 6% of local lesions (Fig. 3A), suggesting that the activity of AU1 as a recombination hotspot was influenced by R′. Alternatively, the low recombination activity of AU1 in the absence of R′ was due to positional effect, i.e., the putative influence of the upstream neighboring sequences that replaced R′ in RNA2 and RNA3.

To test for a possible positional effect, AU1 was introduced into a new downstream location in RNA2 and RNA3, generating constructs N2-AU1 RNA2 and PN-AU1N RNA3. N2-AU1 RNA2 has the AU1 40 nt closer to the 3′ terminus compared to DIC-AU1, and PN-AU1N RNA3 contains 19 nt more of RNA3-derived sequence than PN-AU1 (Fig. 3A and B). Figure 3B shows that PN-AU1N supported low homologous recombination activity (14 to 22%) when coinoculated with DIC-AU1 or N2-AU1 RNA2. This result indicates that AU1 was only partially active in homologous recombination without R′ and that a positional effect was not likely contributing to the low incidence of homologous recombination.

To determine whether R′ must be present in both RNA substrates to enhance recombination in downstream AU-rich sequences, two RNA2-RNA3 combinations with different inserts were tested: DIC-R′+AU1 RNA2 and PN-AU1 RNA3; and DIC-AU1 RNA2 and PN-R′+AU1 RNA3 (Fig. 3C and D). In the former combination, R′ was present only in RNA2, while in the latter, R′ was present only in RNA3. The AU1 was common to both RNA2 and RNA3. The incidences of homologous recombination were 6% for DIC-R′+AU1 RNA2 and PN-AU1 RNA3 and 17% for DIC-AU1 RNA2 and PN-

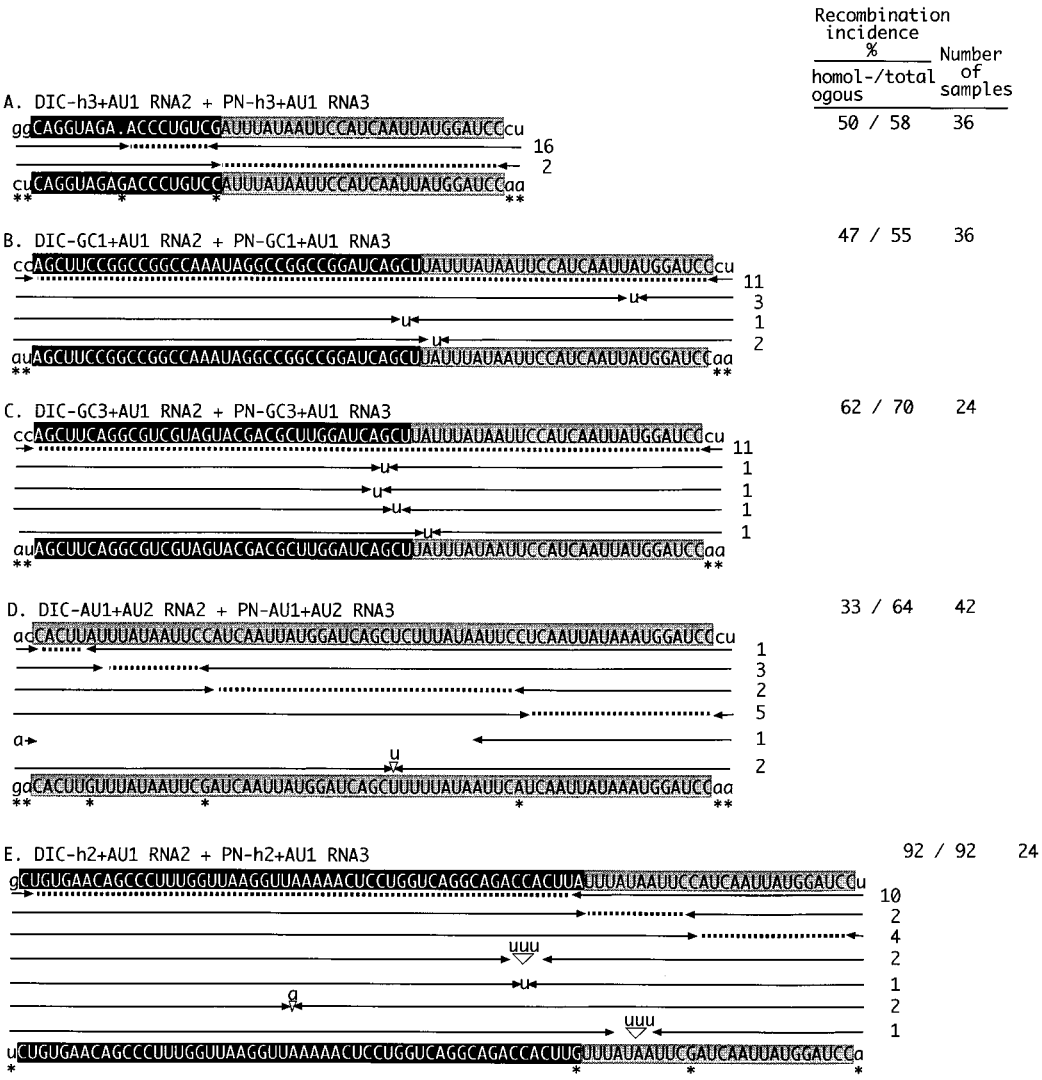

FIG. 4. Distribution of crossover sites in homologous recombinant RNA3 molecules and the incidence of recombination obtained with pairs of RNA2-RNA3 constructs having common R′s replaced with various sequences (shown in black boxes) in both RNAs. The total numbers of samples analyzed and other features are as described in the legend to Fig. 2.

R′+AU1 RNA3 [Fig. 3C and D]). In addition, the majority of crossovers were imprecise. This result shows that R′ needs to be present at upstream positions in both recombining RNAs to enhance the frequency of homologous recombination within the AU-rich sequences. Based on this result, it is unlikely that R′ can enhance homologous recombination by serving as an obstacle for the replicase, as we indicated above.

The R′ region is replaceable with viral and nonviral sequences. To test whether sequences other than R′ can increase homologous recombination when present upstream of the AU-rich sequence, three GC-rich sequences, one sequence with close to equal G/C and A/U contents, and one AU-rich sequence were used to replace R′ that has 64% A/U content. Of these sequences, the GC-rich sequences did not support homologous recombination by themselves when present in both RNA2 and RNA3 constructs (31). This group included h3 (an 18-nt-long sequence from the upstream portion of the 3′ noncoding region in RNA3, 61% G/C content [Fig. 1]) and artificial sequences GC1 (37 nt, 68% G/C content) and GC3 (36 nt, 56% G/C content) (Fig. 4B and C). Infections with RNA2 and RNA3 constructs carrying h3 plus AU1 (DIC-h3+AU1 RNA2 and PN-AU1 RNA3 [Fig. 4A]) induced homologous RNA2-RNA3 recombinants mainly within the h3 region in 50% of local lesions. Infections with GC1 plus AU1 or GC3 plus AU1 (DIC-GC1+AU1 RNA2 and PN-GC1+AU1 RNA3 or DIC-GC3+AU1 RNA2 and PN-GC3+AU1 RNA3) resulted in 47 and 62% homologous recombinants (Fig. 4B and C). Thus, three different GC-rich sequence elements increased the incidence and precision of crossover events within or close to the downstream AU1 compared to AU1 alone. These GC-rich sequences functioned almost as efficiently as R′ (75%, DIC-R′+AU1 RNA2 and PN-R′+AU1 RNA3 [Fig. 2B]) as homologous recombination enhancers.

R′ was next replaced with the h2 sequence (54 nt, 52% A/U content), which is derived from the upstream portion of the 3′ noncoding region in RNA2 (Fig. 1). The homologous recombination incidence was 92% for constructs that carried h2 plus AU1 (DIC-AU1 RNA2 and PN-h2+AU1 RNA3 [Fig. 4E]), an increase by 42% compared with h2 alone (without the AU1 and R′ elements [31]). Most of the crossover events were

within or close to AU1. The results obtained for h2 plus AU1 are similar to those obtained for R′ plus AU1 (Fig. 2B). Thus, homologous recombination activity of sequences that have near equal G/C and A/U contents or are GC-rich can increase homologous recombination when located upstream of an AU1 region.

We next tested if an AU-rich sequence (AU1, 75% A/U content) can enhance the homologous recombination activity of downstream AU2. Plants inoculated with constructs DIC-AU1+AU2 RNA2 and PN-AU1+AU2 RNA3 had a homologous recombination incidence of 33% (Fig. 4D), with the crossover events occurring within both the AU1 and AU2 sequences. Since AU1 alone can support nearly 14% recombination (Fig. 3B), the observed 19% increase in the homologous recombination incidence is likely due to the increased length of the AU1+AU2 region (from 28 to 65 nt [Fig. 4D]) compared to AU1 alone. This result indicates that the upstream AU1 did not effectively enhance recombination activity of the downstream AU2.

AU-rich sequences are required on both RNAs for efficient recombination. To test whether AU-rich sequences need to be present in both recombining RNAs, plant were inoculated with pairwise combinations of RNA2s and RNA3s with an upstream GC1 and either a downstream AU1 (75% A/U content) or a downstream GC-rich sequence (52% G/C content in DIC-GC1 RNA2 and 64% in PN-GC1 RNA3) (Fig. 5A and B). Infections with DIC-GC1+AU1 RNA2 and PN-GC1 RNA3 or DIC-GC1 RNA2 and PN-GC1+AU1 RNA3 induced less than 10% homologous recombinants. This result suggested that the AU1 must occur on both recombining RNAs to support efficient recombination.

To test if sequence similarity of the AU-rich regions is required for efficient homologous recombination, we constructed several RNA2 and RNA3 derivatives with 28- to 31-nt-long, unrelated AU-rich sequences downstream of the common R′ (Fig. 5C to F). DIC-H39 RNA2 and PN-R′+AU1 RNA3, which had heterologous AU-rich sequences with 61 and 75% A/U content, respectively, generated 79% homologous recombinants (Fig. 5C). In addition, RNA2-RNA3 homologous recombinants were found with high frequency when the downstream sequence was U rich in RNA2 and AU rich in RNA3 (63% recombination incidence in the case of DIC-R′+AUU RNA2 and PN-R′+AU1 RNA3 [Fig. 5D]) or when the downstream sequence was A rich in RNA3 and AU rich in RNA2 (81% for DIC-R′+AU1 RNA2 and PN-R′+A20 RNA3 and 72% for DIC-R′+AU3 RNA2 and PN-R′+A20 RNA3 [Fig. 5E and F]). These experiments demonstrate that high sequence similarity between the AU-rich sequences is not required to support efficient homologous recombination. Also, similar to the results obtained using homologous AU-rich sequence downstream from the R′, most of the junctions were located within the 5′ portions of the heterologous AU-rich regions in both RNAs. The heterologous AU-rich sequences supported higher levels of imprecise homologous recombinants than the homologous AU-rich sequences.

AU-rich sequence in RNA3 can participate in inefficient, nontargeted recombination with RNA1. In addition to the above-described targeted, homology-driven RNA2-RNA3 recombination, we have observed the accumulation of nontargeted RNA1-RNA3 recombinants. The latter, referred to as background recombinants, together with the homologous RNA2-RNA3 recombinants make up the total recombination incidence in Fig. 2 to 5. Sequencing through the junction sites in nontargeted RNA1-RNA3 recombinants revealed that they were located within AU-rich sequences in RNA3 more frequently than in other parts of the 3′ noncoding regions (Fig. 6). The junction sites in RNA1 also tended to cluster in the vicinity of an AU-rich sequence. Thus, it is possible that the generation of background recombinants was facilitated by the AU-rich sequences. It is important to note, however, that besides the variable frequency, most of the nontargeted recombinants accumulated late (21 days postinoculation) during the infection (data not shown).

The occurrence of background recombinants may have led to underestimation of the frequency of homologous RNA2-RNA3 recombination in the experiments shown in Fig. 2 to 5. The background recombinants can be generated by recombination between RNA3 and either wt RNA1 or the DIC series of RNA2 (due to the presence of RNA1-derived region at the 3′ end of the DIC series of RNA2 [Fig. 1]). To decrease the frequency of the generation of background recombinants, the RNA1-derived region in DIC-R′+AU1 RNA2 was replaced with the 3′ end of wt RNA2, leading to construct N2-R′+AU1 RNA2 (Fig. 1). The incidence of background recombinants was low (11%) in N2-R′+AU1 RNA2 and PN-AU1N RNA3 infections compared to that observed in DIC-R′+AU1 RNA2 and PN-AU1N RNA3 infections (44%) (Fig. 3C), yet the incidences of targeted homologous RNA2-RNA3 recombination in the two systems were the same (6%). Similarly, the frequency of background recombinants was reduced to 3% from 36%, while that of homologous recombinants remained similar, in infections with N2-AU1 RNA2 that lacked R′ and the RNA1-derived sequences and PN-AU1N RNA3 compared to infections with DIC-AU1 RNA2 and PN-AU1N RNA3 (Fig. 3B). Thus, reducing the frequency of background recombinants did not influence significantly the frequency of homologous recombinants. We conclude that the incidence of homologous RNA2-RNA3 recombinant isolation (as shown in Fig. 2 to 5) reflects the frequency of their generation in local lesions of *C. quinoa.*

Growth characteristics of the parental and recombinant RNAs. Different recombinant RNA3s might have had different growth advantages which can influence the frequency of their isolation. To test this possibility, we reconstructed five different precise homologous recombinant RNA3s. Of these, three were isolated frequently de novo: rec-R′ RNA3 (Fig. 2A), rec-R′+AU1 RNA3 (Fig. 2B), and rec-R′+AU3 RNA3 (Fig. 2E). The remaining two (designated rec-AU1 RNA3 and rec-AU1N RNA3) represented homologous recombinants that could potentially be generated in infections, but they were not detected in experiments shown in Fig. 3A and B. Like the corresponding de novo recombinants, these reconstructed RNA3 molecules contained the targeted region (R′ and/or AU1 or AU3) derived entirely from RNA3 and the downstream 236 bp 3′ noncoding region derived from DIC-R′+AU1 RNA2 segment (shown schematically in Fig. 1). We found that all five reconstructed recombinant RNA3s accumulated to comparable levels in local lesions of *C. quinoa* after coinoculation with wt RNA1 and either DIC-R′, DIC-R′+AU1, or DIC-R′+AU3 RNA2 (Fig. 7). Also, the levels of accumulation of RNA2 components in these five different combinations of RNA2s and RNA3s were comparable. Sequencing of the 3′ ends in six progeny RNA3s, each derived from a separate local lesion obtained with DIC-R′+AU1 and rec-R′+AU1, demonstrated that the R′+AU1 region was maintained in the RNA3 molecules. These data suggest that if these recombinants were generated with similar frequencies, they should have been detected with comparable frequencies in separate experiments. Apparently, the observed differences in the incidence of homologous recombination were not due to altered selective advantages (disadvantages) of the parental BMV RNAs. Similar data for RNA2 and RNA3 molecules

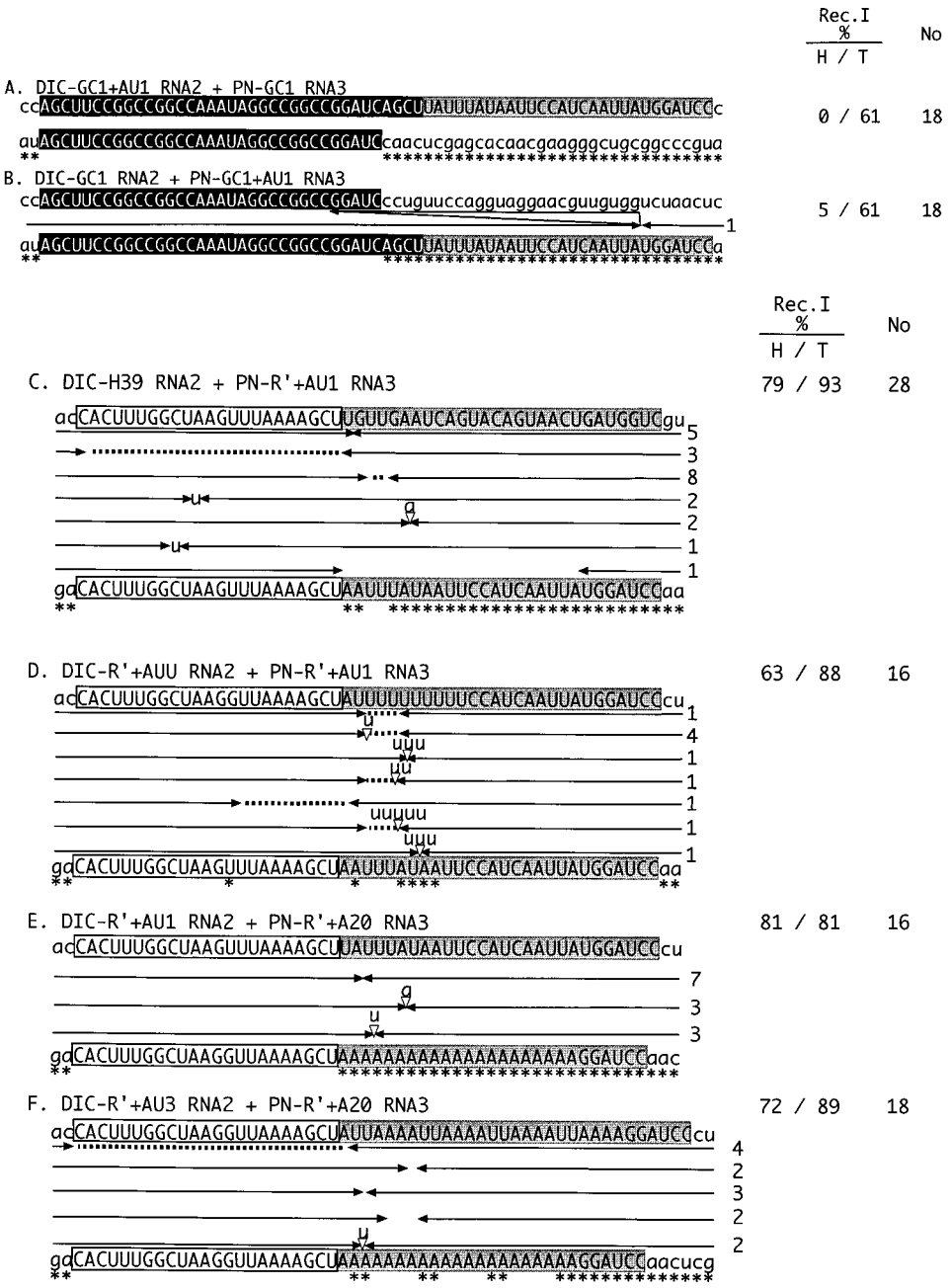

FIG. 5. Incidence of recombination and distribution of crossover sites in homologous recombinant RNA3 molecules obtained with pairs of RNA2-RNA3 constructs having heterologous downstream sequences with average or high A/U content. The total numbers of samples analyzed and other features are as described in the legends to Fig. 2 to 4.

with mutagenized R′ have been published previously (30). We conclude that the results of the experiments described in this report reflect the frequency of homologous recombination in the targeted region.

The possibility that the recombinants represent RT-PCR artifacts was excluded by the fact that the recombinant-size RNA3 was detected by Northern blotting of total RNA extracts from local lesions obtained with DIC-R′+AU1 RNA2 and PN-R′+AU1 RNA3 (data not shown). Also, control RT-PCR amplifications of mixtures of in vitro-transcribed wt RNA1, DIC-R′+AU1 RNA2, and PN-R′+AU1 RNA3 generated parental-size, but not the recombinant-size, RNA3-specific cDNAs (data not shown).

DISCUSSION

In this report, we demonstrate that homologous recombination hotspots can be generated in BMV at short artificial AU-rich sequences present in both recombining RNAs. These artificial AU-rich sequences were favored during recombination over a BMV-derived natural hotspot sequence, such as R′. The ability of the AU-rich sequences to support homologous re-

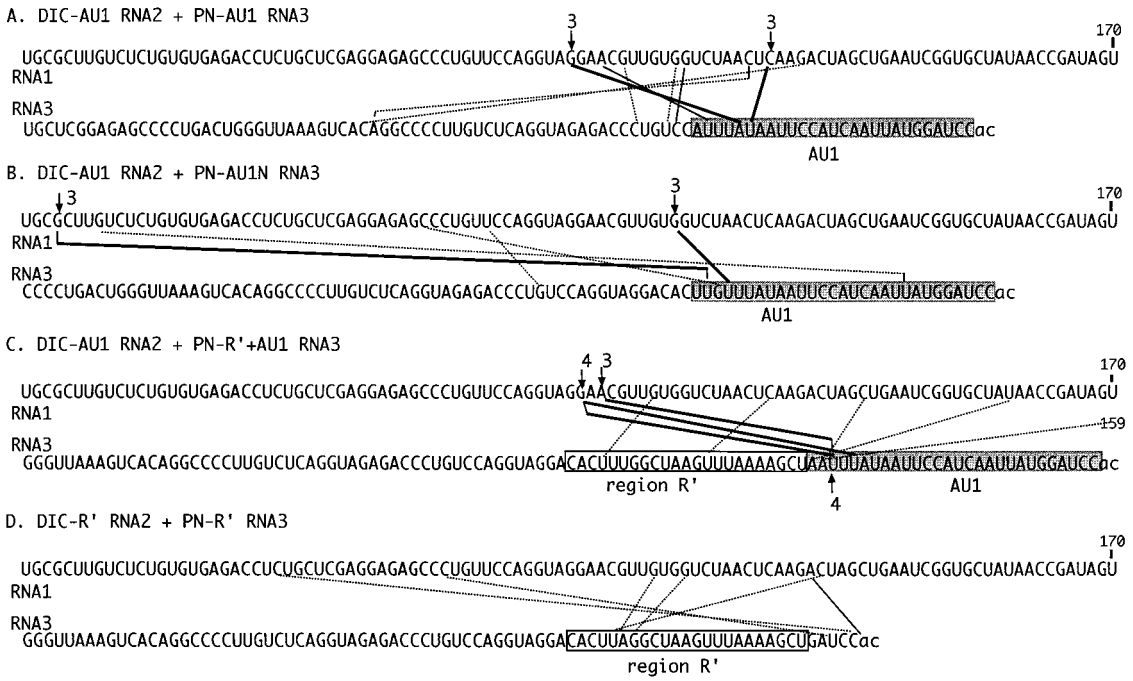

FIG. 6. Locations of crossover sites in RNA1-RNA3 nontargeted (background) recombinants. Upper lines represent RNA1 (positions 170 to 273, counted from the 3′ end), while the lower line represents RNA3 3′ noncoding sequences (R′ is boxed, and the AU1 cassette is shaded). For each recombinant, the last nucleotide of RNA3 preceding the recombination junction and the first nucleotide of RNA1 sequence following the recombination junction are connected by lines between the two RNA sequences. Broken lines indicate crossovers that were identified once, thin solid lines depict crossovers found twice, and thickest lines represent those identified in three or four local lesions (as indicated by arrows and numbers).

combination was increased markedly with common upstream regions of higher G/C content.

The criteria for selecting the upstream and downstream elements were to (i) keep the length comparable to that of R′, (ii) use different primary sequences with variable percentages of AU and GC, and (iii) avoid homopolymer stretches that might have unusual secondary structures. Six and four different upstream and downstream sequences, respectively, were tested. Using the same downstream AU-rich element, we found that three GC-rich and two moderately AU-rich (up to 61% A/U) sequences enhanced the frequency of recombination within or adjacent to the AU-rich downstream element. In contrast, a highly AU-rich (74% A/U content) upstream common sequence did not support high-frequency recombination within the downstream AU-rich element. All four downstream AU-rich sequences tested supported some homologous recombination, suggesting that the nucleotide composition rather than the primary sequence of the targeted region was important for targeting recombination to the region. We also found that while the upstream region must bear high sequence similarity, the downstream region can be heterologous in the recombining RNAs.

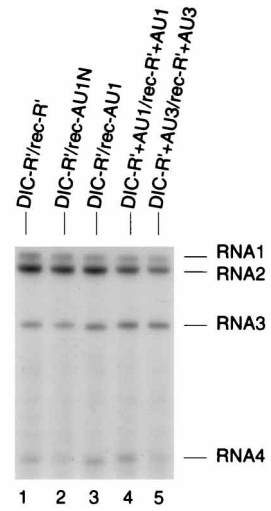

FIG. 7. Analysis of accumulation levels of various parental RNA2 mutants and reconstructed RNA3 recombinants in whole plants, as determined by Northern blotting. Leaves of *C. quinoa* were inoculated with a mixture of in vitro-transcribed wt RNA1 and one of the RNA2 and RNA3 mutants (as shown above the lanes). *C. quinoa* plants were incubated for 10 days. Total RNA extracts were isolated from single local lesions and separated by electrophoresis in a 1% agarose gel. The RNA was transferred to a nylon membrane and probed with a 200-nt-long ^{32}P-labeled RNA probe specific for the 3′ noncoding region of RNA1 to RNA4 as described in Materials and Methods.

We have analyzed the stem-loop and pseudoknot structures of the upstream GC-rich and downstream AU-rich regions. Computer-predicted secondary structures varied markedly among the constructs that supported recombination with similar frequencies (data not shown). Therefore, together with our previous data (28, 30), we do not find any obvious role for the secondary structure elements in the targeted region during the selection of homologous junction sites.

The lack of requirement for a particular sequence motif or RNA structure or a given position within the 3′ noncoding region suggests that the presence of two adjacent regions differing in nucleotide content (upstream common GC rich or moderately AU rich and downstream AU rich) is the significant factor that generates a homologous recombination hotspot. We propose that the common upstream GC-rich or mod-

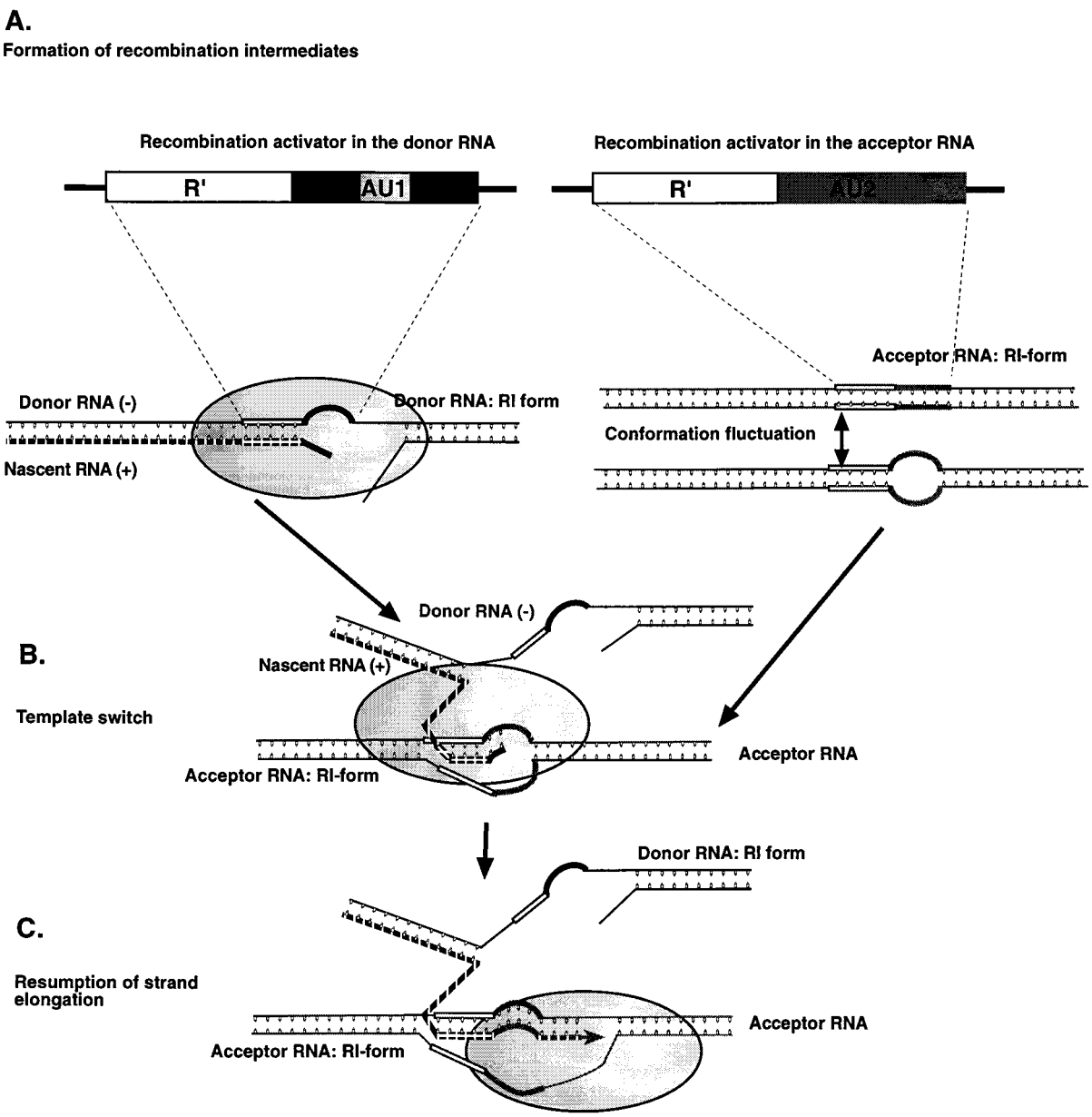

FIG. 8. Diagrammatic representation of a processive template-switching model explaining the formation of homologous recombination hotspots within the recombination activator sequences (e.g., R′+AU1 sequences). (A) According to the model, template switching of the BMV replicase occurs during positive-strand synthesis. Though localized double-stranded RIs are shown, the existence of single-stranded RNAs with negative polarity is also possible (not shown). The weak base pairing within the AU-rich region (shown on the left side of the diagram with a black line) can facilitate the release of the 3′ end of the incomplete nascent RNA. The weak base pairing within the AU-rich region can also facilitate the temporary formation of a bubble structure in the RI of the acceptor strand (shown with gray lines on the right side of the diagram). The replicase (represented by a large shadowed ellipse) pauses on the donor strand at the AU-rich region, and the very 3′ end of the nascent strand disengages from the original template strand. (B) The released 3′ end of the nascent strand hybridizes to the acceptor strand facilitated by the bubble structure. Hybridization at the upstream located R′ (shown by empty boxes) stabilizes the recombination intermediate. (C) The viral replicase resumes chain elongation on the acceptor strand (shown by an arrowhead). This leads to the formation of homologous recombinant RNA3s.

erately AU-rich element together with the AU-rich downstream element forms a homologous recombination activator. To facilitate homologous recombination, the homologous recombination activator sequence should be present in both recombining RNAs, but sequence similarity is required only for the upstream element.

Our data give insight into the mechanism of homologous recombination in BMV. The requirement for the presence of a short common GC-rich sequence upstream of an AU-rich cassette in both RNA2 and RNA3 cannot be easily described by replicase-switching events that occur between the RNA templates during negative-strand synthesis. This is because if template switching occurs within the favored AU-rich region (most of the crossovers clustered at or around the 5′ portion of the AU-rich region, spanning approximately 5 to 10 nt), then the negative-stranded nascent RNA would not contain any sequences from the upstream region (e.g., R′ sequence). Why then is the upstream sequence required during the crossover

events? One possibility is that a common upstream sequence facilitates interactions between donor and acceptor strands via RNA-RNA, RNA-protein, or protein-protein interactions. This, however, implies a specific sequence and cannot easily explain the observed recombination enhancer-like activity of five different upstream sequences. Also, it is difficult to explain how heterologous AU-rich sequences would facilitate targeting the crossover sites to the AU-rich sequences (Fig. 5C to E), because the nascent minus strands would have no complementary sequence to the acceptor plus strands in the crossover region.

Taking the available data together, we propose that most of the homologous recombination events occur during positive-strand synthesis (Fig. 8). According to this model, the AU-rich sequence in the donor RNA (i.e., negative strand of RNA3) has two functions. First, it serves as a putative pause site for the replicase. Indeed, pausing within U-rich sequences has been described for prokaryotic RNA polymerases (24) and for eukaryotic RNA polymerase I (22). Also, AU-rich regions might be more accessible to single-stranded nicking. This could then promote template switching of the replicase, as has been demonstrated for reverse transcriptase reactions (12, 23, 32, 44). Second, the AU-rich region might promote more efficient release of the 3′ end of the nascent strand (launching event) from the template strand due to weak A-U base pairings with the template strand. The role of AU-rich sequences in the release of RNA transcripts during transcription termination by RNA polymerase I is well defined (22).

According to our model, the release of the 3′ end of the aborted nascent strand from the donor template strand is followed by the association (docking event) of the nascent strand with the acceptor strand (here to the negative strand of RNA2). This could be facilitated by the G and C nucleotides within the upstream GC-rich element in the recombination activator by stabilizing the base pairing between these RNAs. This proposed base-pairing step explains why high sequence similarity in the GC-rich upstream region, but not in the downstream AU-rich region, is required to produce a homologous recombination hotspot.

According to the model, AU-rich sequences alone are less efficient in securing the docking of the 3′ end of the nascent strand at the acceptor strand, while GC-rich sequences alone are less efficient in releasing the 3′ end of the aborted nascent strand from the template strand. Indeed, even 65-nt-long common AU-rich sequences supported only a moderate level of homologous recombination (Fig. 4D). Also, highly AU-rich sequences in the absence of the upstream common region generated frequently imprecise recombinants with short deletions or insertions or mismatched and nontemplated nucleotides at the crossover junction in the AU-rich region, possibly due to misannealing between the nascent and the acceptor RNA strands (Fig. 3 and reference 30). On the other hand, purely GC-rich sequences may inhibit the dissociation step. Accordingly, we did not find homologous crossovers within common GC-rich sequences in BMV (Fig. 5A and B and reference 31). Also, A to C(G) mutagenesis of a hotspot region reduced the incidence of homologous recombination and changed the distribution of crossover sites in BMV (28, 31).

The structure of the BMV RNA intermediates during positive-strand synthesis is not known. It seems plausible that the target region of the negative-stranded acceptor RNA is double stranded (as part of a localized replication intermediate [RI] formed between the positive and negative strands [4, 34]). The interstrand base pairing in the RIs would explain why we could not find a definite role for the secondary structure of the target region in homologous recombination. On the other hand, if the target region in the acceptor RNA is double stranded, the interaction between the 3′ end of the nascent strand and the target region would be difficult. We propose that breathing (i.e., local conformation fluctuation between base-paired and locally non-base-paired [bubble] forms) can occur within the less stable AU-rich region (Fig. 8). Such a temporary bubble structure might then facilitate the docking event by allowing local base-pairing between the nascent and acceptor strands (Fig. 8). This model explains why (i) heterologous AU-rich downstream sequences in the acceptor RNA facilitate crossover events by promoting the formation of the bubble structure, while (ii) the absence of AU-rich sequence (i.e., the bubble structure) inhibits homologous crossovers (Fig. 5A). Further experiments are needed to demonstrate the structure of the RIs.

In conclusion, our data suggest that homologous crossovers occur during positive-strand synthesis. However, it has been demonstrated previously that homologous recombination also occurs during negative-strand synthesis, but the generation of recombinants was less efficient (28, 30). Indeed, we found that the replication-incompetent form of PN-R′+AU1 RNA3 (which lacked the entire 3′ minus-strand initiation promoter) generated homologous recombinants approximately 100 times less frequently than the replication-competent PN-R′+AU1 RNA3 (data not shown). This might be due to a preference for crossovers to occur during positive-strand synthesis and/or fast degradation of nonreplicating RNA3 molecules. Further experiments will explore the role of positive and negative strands in recombination.

It is likely that recombination activator-like sequences can function as homologous recombination hotspots in other RNA viruses. If so, artificial homologous crossover sites can be generated in different viruses. This, in turn, can facilitate the development of recombinant RNA technology to fuse different RNA molecules together in vivo.

ACKNOWLEDGMENTS

We thank M. Figlerowicz, M. Graves, R. Olsthoorn, J. Pogany, A. Simon, and A. White for comments and discussions and for helping to improve the manuscript.

This work was supported by grants from the National Institute for Allergy and Infectious Diseases (3RO1 AI26769) and National Science Foundation (MCB-9630794) and by the Plant Molecular Biology Center at Northern Illinois University.

REFERENCES

1. **Ahlquist, P.** 1992. Bromovirus RNA replication and transcription. Curr. Opin. Genet. Dev. **2:**71–76.
2. **Ahlquist, P., R. Dasgupta, and P. Kaesberg.** 1984. Nucleotide sequence of the brome mosaic virus genome and its implications for viral replication. J. Mol. Biol. **172:**369–383.
3. **Allison, R. F., M. Janda, and P. Ahlquist.** 1989. Sequence of cowpea chlorotic mottle virus RNAs 2 and 3 and evidence of a recombination event during bromovirus evolution. Virology **172:**321–330.
4. **Andino, R. G. E. Rieckhof, and D. Baltimore.** 1990. A functional ribonucleoprotein complex forms around the 5′ end of poliovirus RNA. Cell **63:**369–380.
5. **Bujarski, J. J., and A. M. Dzianott.** 1991. Generation and analysis of nonhomologous RNA-RNA recombinants in brome mosaic virus: sequence complementarities at crossover sites. J. Virol. **65:**4153–4159.
6. **Bujarski, J. J., and P. Kaesberg.** 1986. Genetic recombination between RNA components of a multipartite plant virus. Nature **321:**528–531.
7. **Bujarski, J. J., and P. D. Nagy.** 1994. Genetic RNA-RNA recombination in positive-stranded RNA viruses of plants. p. 1–24. *In* J. Paszkowski (ed.), Homologous recombination in plants. Kluwer Academic Publisher, Dordrecht, The Netherlands.
8. **Bujarski, J. J., P. D. Nagy, and S. Flasinski.** 1994. Molecular studies of genetic RNA-RNA recombination in brome mosaic virus. Adv. Virus Res. **43:**275–302.
9. **Carpenter, C. D., J.-W. Oh, C. Zhang, and A. E. Simon.** 1995. Involvement of a stem-loop structure in the location of junction sites in viral RNA

recombination. J. Mol. Biol. **245:**608–622.
10. **Cascone, P. J., C. D. Carpenter, X. H. Li, and A. E. Simon.** 1990. Recombination between satellite RNAs of turnip crinkle virus. EMBO J. **9:**1709–1715.
11. **Cascone, P. J., T. F. Haydar, and A. E. Simon.** 1993. Sequences and structures required for recombination between virus-associated RNAs. Science **260:**801–805.
12. **Coffin, J. M.** 1979. Structure, replication, and recombination of retrovirus genomes: some unifying hypotheses. J. Gen. Virol. **42:**1–26.
13. **Dolja, V. V., and J. C. Carrington.** 1992. Evolution of positive-strand RNA viruses. Semin. Virol. **3:**315–326.
14. **Goldbach, R., O. Le Gall, and J. Wellink.** 1991. Alpha-like viruses in plants. Semin. Virol. **2:**19–25.
15. **Janda, M., R. French, and P. Ahlquist.** 1987. High efficiency T7 polymerase synthesis of infectious RNA from cloned brome mosaic virus cDNA and effects of 5′ extensions of transcript infectivity. Virology **158:**259–262.
16. **Jarvis, T. C., and K. Kirkegaard.** 1991. The polymerase in its labyrinth: mechanisms and implications of RNA recombination. Trends Genet. **7:**186–191.
17. **King, A. M. Q.** 1988. Genetic recombination in positive strand RNA viruses, p. 149–185. *In* E. Domingo, J. J. Holland, and P. Ahlquist (ed.), RNA genetics, vol. II. CRC Press, Boca Raton, Fla.
18. **Kirkegaard, K., and D. Baltimore.** 1986. The mechanism of RNA recombination in poliovirus. Cell **47:**433–443.
19. **Kroner, P., D. Richards, P. Traynor, and P. Ahlquist.** 1989. Defined mutations in a small region of the brome mosaic virus 2a gene cause diverse temperature-sensitive RNA replication phenotypes. J. Virol. **63:**5302–5309.
20. **Kuge, S., I. Saito, and A. Nomoto.** 1986. Primary structure of poliovirus defective-interfering particle genomes and possible generation mechanisms of the particles. J. Mol. Biol. **192:**473–487.
21. **Lai, M. C. M.** 1992. RNA recombination in animal and plant viruses. Microbiol. Rev. **56:**61–79.
22. **Lang, W. H., and R. H. Reeder.** 1995. Transcription termination of RNA polymerase I due to a T-rich element interacting with Reb1p. Proc. Natl. Acad. Sci. USA **92:**9781–9785.
23. **Luo, G., and J. Taylor.** 1990. Template switching by reverse transcriptase during DNA synthesis. J. Virol. **64:**4321–4328.
24. **Macdonald, L. E., Y. Zhou, and W. T. McAllister.** 1993. Termination and slippage by bacteriophage T7 RNA polymerase. J. Mol. Biol. **232:**1030–1047.
25. **Marsh, L. E., G. P. Pogue, C. C. Huntley, and T. C. Hall.** 1991. Insight to replication strategies and evolution of (+) strand RNA viruses provided by brome mosaic virus. Oxford Surv. Plant Mol. Cell. Biol. **7:**297–334.
26. **Nagy, P. D., and J. J. Bujarski.** 1992. Genetic recombination in brome mosaic virus: effect of sequence and replication of RNA on accumulation of recombinants. J. Virol. **66:**6824–6828.
27. **Nagy, P. D., and J. J. Bujarski.** 1993. Targeting the site of RNA-RNA recombination in brome mosaic virus with antisense sequences. Proc. Natl. Acad. Sci. USA **90:**6390–6394.
28. **Nagy, P. D., and J. J. Bujarski.** 1995. Efficient system of homologous RNA recombination in brome mosaic virus: sequence and structure requirements and accuracy of crossovers. J. Virol. **69:**131–140.
29. **Nagy, P. D., A. Dzianott, P. Ahlquist, and J. J. Bujarski.** 1995. Mutations in the helicase-like domain of protein 1a alter the sites of RNA-RNA recombination in brome mosaic virus. J. Virol. **69:**2547–2556.
30. **Nagy, P. D., and J. J. Bujarski.** 1996. Homologous RNA recombination in brome mosaic virus: AU-rich sequences decrease the accuracy of crossovers. J. Virol. **70:**415–426.
31. **Nagy, P. D., and J. J. Bujarski.** Unpublished data.
32. **Peliska, J. A., and S. J. Benkovic.** 1994. Fidelity of *in vitro* DNA strand transfer reactions catalyzed by HIV-1 reverse transcriptase. Biochemistry **33:**3890–3895.
33. **Pogany, J., J. Romero, Q. Huang, J.-Y. Sgro, H. Shang, and J. J. Bujarski.** 1995. *De novo* generation of defective interfering-like RNAs in broad bean mottle bromovirus. Virology **212:**574–586.
34. **Pogue, G. P., and T. C. Hall.** 1992. The requirement for a 5′ stem-loop structure in brome mosaic virus replication supports a new model for viral positive-strand RNA initiation. J. Virol. **66:**674–684.
35. **Rao, A. L. N., and T. C. Hall.** 1990. Requirement for a viral *trans*-acting factor encoded by brome mosaic virus RNA-2 provides strong selection in vivo for functional recombinants. J. Virol. **64:**2437–2441.
36. **Rao, A. L. N., and T. C. Hall.** 1993. Recombination and polymerase error facilitate restoration of infectivity in brome mosaic virus. J. Virol. **67:**969–979.
37. **Rao, A. L. N., B. P. Sullivan, and T. C. Hall.** 1990. Use of *Chenopodium hybridum* facilitates isolation of brome mosaic virus RNA recombinants. J. Gen. Virol. **71:**1403–1407.
38. **Romanova, L. I., V. M. Blinov, E. A. Tolskaya, E. G. Viktorova, M. S. Kolesnikova, E. A. Guseva, and V. I. Agol.** 1986. The primary structure of crossover regions of intertypic poliovirus recombinants: a model of recombination between RNA genomes. Virology **155:**202–213.
39. **Sambrook, J., E. F. Fritsch, and T. Maniatis.** 1989. Molecular cloning: a laboratory manual, 2nd ed. Cold Spring Harbor Laboratory, Cold Spring Harbor, N.Y.
40. **Simon, A. E., and J. J. Bujarski.** 1994. RNA-RNA recombination and evolution in virus infected plants. Annu. Rev. Phythopathol. **32:**337–362.
41. **Strauss, J. H., and E. G. Strauss.** 1988. Evolution of RNA viruses. Annu. Rev. Microbiol. **42:**657–683.
42. **White, K. A., and T. J. Morris.** 1994. Recombination between defective tombusvirus RNAs generates functional hybrid genomes. Proc. Natl. Acad. Sci. USA **91:**3642–3646.
43. **White, K. A., and T. J. Morris.** 1995. RNA determinants of junction site selection in RNA virus determinants and defective interfering RNAs. RNA **1:**1029–1040.
44. **Wu, W., B. M. Blumberg, P. J. Fay, and R. A. Bambara.** 1995. Strand transfer mediated by human immunodeficiency virus reverse transcriptase *in vitro* is promoted by pausing and results in misincorporation. J. Biol. Chem. **270:**325–332.
45. **Zimmern, D.** 1988. Evolution of RNA viruses, p. 211–240. *In* J. J. Holland, E. Domingo, and P. Ahlquist (ed.), RNA genetics. CRC Press, Boca Raton, Fla.